Timber floors in Old Buildings

Study of a Reinforcement Solution

Diogo Silva Chen

DECivil, Instituto Superior Técnico, Universidade de Lisboa, Portugal

Abstract: Old Unreinforced Masonry Buildings (URM) when affected by horizontal dynamic actions, such as seismic action, depend significantly on the stiffness and strength of the floors and on the existing connections between the floors and the masonry walls. Although, in these types of buildings, the floor is usually made of timber beams and boards which are poorly connected between themselves and with the walls. These aspects prevent the building from distributing inertia forces to vertical elements properly. It is therefore proposed a type of reinforcement consisting of wood-based panels, OSB, in order to improve the in-plane stiffness and strength of existing old floors. The reinforcement is based on a timber floor executed with traditional construction techniques. The reinforcement was analyzed through numerical models. The connections were modeled based on laboratory cyclic tests of three different types: nailed, screwed and glued. Nailed connections showed higher stiffness and strength alongside with higher dissipation of energy per cycle compared to screwed connections. Glued connections showed the highest level of stiffness, although, it was not possible to draw conclusions regarding its strength. Various configurations of the reinforcement were modelled to perform a parametric analysis. Forty different models where created changing the spacing between connectors and the number of panel's divisions as well applying glued boards to eliminate joints. Among the different variants, only eight revealed adequate strength and stiffness with similar results compared to other reinforcement solutions with higher costs.

Keywords: Timber floors; Seismic reinforcement; In-plane stiffness; In-plane strength; Timber-to-timber connections

1. Introduction

Seismic activity in mainland Portugal is recuring with occurrences mainly in the south and center of the country. In Lisbon specifically, housing is mostly composed of 38% of buildings built prior to 1945 (Censos 2011) and most of them have historical and patrimonial value. Also, the majority of these buildings are made of unreinforced masonry (URM) and timber floors.

URM buildings when affected by horizontal dynamic actions rely on the floors as distributive elements of these forces to the masonry walls and so guarantee a global behavior of the building structure and not contributing to the overturning of individual walls. Although, old timber floors show little in-plane stiffness and strength and no proper connections with the masonry walls. These aspects do not contribute to a box behavior of the structure.

In order to improve the tridimensional behavior of URM buildings, it is necessary to increase the in-plane stiffness and strength of the floors but also enhance the quality of the connections between floors and walls.

Only the reinforcement of the floors in-plane stiffness and strength are studied in this work. The reinforcement is based on oriented strand boards (OSB) panels and was designed for a real scale timber floor made by Fragomeli (2015). A study through non-linear numerical models was carried out.

Three different types of connections (nailed, screwed and glued connections) were tested for dynamic actions to model their behavior.

2. Previous studies

Various studies were carried out with the end goal of improving the in-plane stiffness of old timber floors. Fragomeli (2015) studied the effect of nails' disposition on the in-plane stiffness. The reinforcement consisted of two nails per plank arranged

to maximize the distance between each one and consequently increase the rotation stiffness between board and beams. Corradi *et al.* (2006) also studied the influence of connections within the timber floors adding two nails in the middle of planks. Although both these authors reached lower values of in-plane stiffness.

Nunes *et al.* (2020) proposed a reinforcement consisting of a reticulated steel structure screwed to the existing floor resulting on an increase of the in-plane stiffness of twenty seven times more compared to the unreinforced floor. A similar study was carried out by Piazza *et al.* (2008) which achieved an increase of in-plane stiffness around eleven times more. Valluzzi *et al*. (2010) studied the effects of a single steel bar arranged diagonally to the timber floor and found that the increase of in-plane stiffness to be around five times higher than the original value. Though Valluzzi *et al*. (2010) only carried out monotonic tests and advises to apply a steel bar on both diagonals.

On another hand, timber-based reinforcements were also studied by Corradi *et al.* (2006), Piazza *et al.* (2008), Valluzzi *et al*. (2010), and Brignola *et al.* (2012). Corradi *et al.* (2006) applied one layer of planks perpendicular to the original planks with and without glass fibers reinforced polymers (GFRP) as strips or as a mesh. The additional planks increased the in-plane stiffness in around four times, but the addition of GFRP improved the reinforcement in seven times. Similarly, Valluzzi *et al*. (2010) studied the effect of two layers of planks arranged in 45º with the original planks which resulted of an increase of twenty one times compared to the unreinforced floor. Piazza *et al.* (2008) noted the highest increase of in-plane stiffness (around eighty six times more) when three panels of plywood were applied to the original floor. This result was even higher than a concrete slab solution studied by the same author. Brignola *et al.* (2012) proposed the addition of plywood panels in one layer and studied the effects that different boundary conditions and a steel frame around the diaphragm perimeter had on the reinforcement. Brignola *et al.* (2012) noted that both the addition of a steel frame and one layer of plywood improve the in-plane stiffness.

3. Testing of timber-to-timber connections

Three different types were tested to characterize the behavior of connections in the proposed reinforcement and in the original floor: nailed, screwed and glued connections. The tests followed the procedure in EN 12512 (2006) which states that a monotonic test in tension must be performed prior to the cycle tests in order to define the yielding point and consequently define the loading protocol. All tests were performed using an equipment INSTRON® (measures forces and imposes displacements) and a video extensometer (measures displacements between targets on the specimens).

The type of wood used had a mean density, $\rho_m^{ens.}$, of 518,5 kg/m^3 and a thickness of 18 mm. The strength class was not stated by the supplier. To prevent the testing pieces from crushing at the attachment zone due to the pressure applied by the equipment, four steel plates of 5 mm thick were screwed to the ends on each side of the piece. The testing pieces followed the 3D scheme on Figure 3.1 which consist of two connections per specimen. Squared section nails with a side dimension of 4 mm were used in order to increase the friction between nail and wood. The screws used had an effective diameter of 4 mm as well. For the glued connection it was used EPICOL-U epoxy resin. Four different testing pieces were executed per type of connection. The first to be tested under a monotonic test in tension and the other three under a cycling test. Table 3.1 shows the name assignment of each.

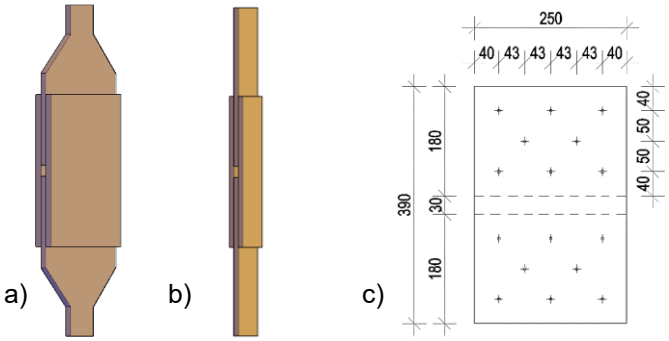

Figure 3.1 – Specimen for a) metal fasteners b) glued connections. c) Disposition metal fasteners (in mm)

Table 3.1 - Name assignment of testing pieces

Name	Type of connection	Type of testing
PREG-C	Nailed	Monotonic
PREG-1		Cyclic
PREG-2		Cyclic
PREG-3		Cyclic
APAR-C	Screwed	Monotonic
APAR-1		Cyclic
APAR-2		Cyclic
APAR-3		Cyclic
COL-C	Glued	Monotonic
COL-1		Cyclic
COL-2		Cyclic
COL-3		Cyclic

3.1. Monotonic testing results

To define the yielding point, a monotonic test was performed on each type of connection (PREG-C, APAR-C and COL-C). Both nailed and screwed connections showed similar yielding displacements hence why it was considered the same loading protocol (Figure 3.2 a)). It was not possible to define the yielding point of glued connections (COL-C) due to testing scheme. The pressure imposed by the equipment led to the rupture of the wood at the supports and not on the connection (Figure 3.2 c)). Although a maximum force of 30,34 kN and a displacement of 0,53 mm was reached. Also, the nailed connection (PREG-C) had a sudden drop of strength due to a mounting screw between the testing piece and the steel plate and not due to the connection itself (Figure 3.2 b)). Each force-displacement curve is on Figure 3.3.

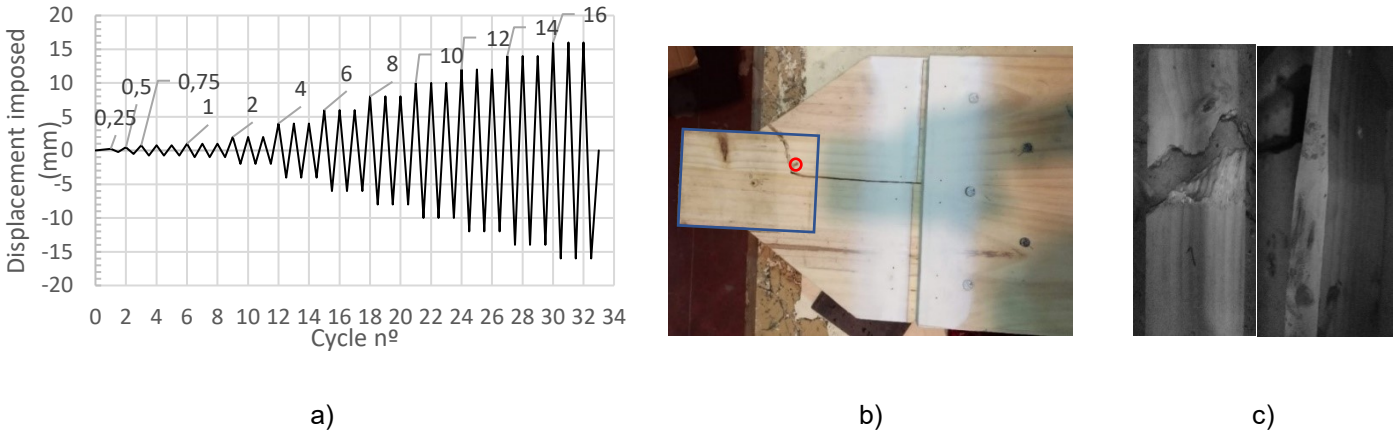

a) b) c)

Figure 3.2 - a) Loading protocol b) Rupture of PREG-C due to mounting screw and place where the steel plate was installed c) Rupture at the support with the equipment of COL-C

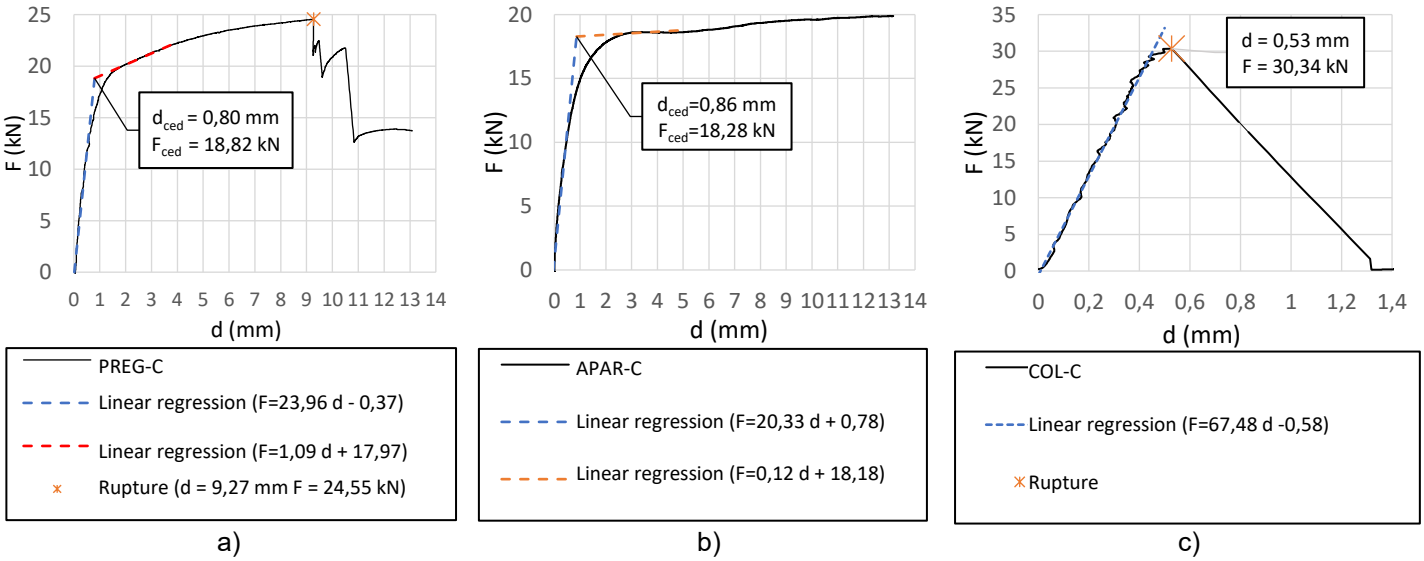

a) b) c)

Figure 3.3 – Monotonic results for a) PREG-C b) APAR-C c) COL-C

3.2. Cyclic testing results

The cyclic tests on metal fasteners (PREG and APAR) revealed symmetric cycles in relation to the load direction. In general, similar values of resistance are reached in both directions and any differences might be caused by possible misalignments in the testing piece and also by slips between the specimen and the equipment.

For cycles prior to the yielding point, it appears that the loss of resistance for the same imposed displacement is around 2% on average, in contrast to the following cycles in which there are losses higher than 10%, mainly in the second cycle of each displacement.

For each level of displacement, it is possible to see the pin

ching effect, common on these types of connections (Figure 3.4 a) and b)). This effect is described as a wider loop in the first cycle followed by narrow loops. This happens due to the wood crushing in the neighboring areas of the connector dissipating more energy. The following loops are then less stiff. Comparing the dissipated energy between nailed and screwed connections, nailed ones show higher values.

In terms of stiffness, screwed connections show lower values per cycle, as shown in Figure 3.5 a). The difference between the two connections may be related to their section geometry and the way they are embedded on wood. The nails used have a squared shape which allows a uniform distribution of stresses and parallel to the wood grain contrary to the circular geometry of the screw section. Also, when the nails are embedded in the wood, stresses are introduced in the hole increasing the friction and thus improving the connection stiffness. On the other hand, in screwed connections, the wood is cut by the connector grooves which then reduces the friction and stiffness of the connection. Although from cycle nº 12 on (imposed displacement of 4 mm), the secant stiffness tends to be the same which might indicate the plasticization of the connectors and so decreasing the importance of wood crushing.

No relevant results in terms of strength were obtained from cyclic tests to glued connections. When the minimum pressure of 20 bar is applied to the test piece in order to attach it to the equipment, the wood is crushed despite the steel plates introduced to reduce this effect. When crushed a wedge is formed which promotes slipping between the equipment and the specimen. Glued connections being more rigid amplify this slipping effect. On Figure 3.5 b), it is possible to observe that, for the first two cycles, there is a greater difference between the displacements imposed by the equipment INSTRON (0,25 mm and 0,50 mm) and the measured displacements between targets when compared to the other connections.

Although the results are not conclusive regarding the maximum strength of glued connections, it appears that the hysteretic curves reveal a similar secant stiffness between tests (Figure 3.5 c)) and with reduced dissipation of energy per cycle. Their behavior is also mainly linear (Figure 3.4 a)).

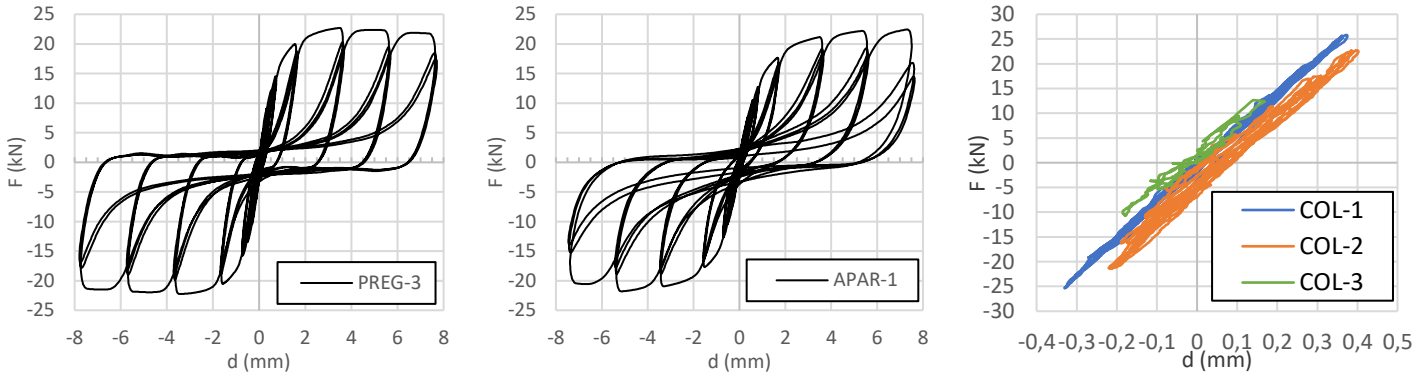

Figure 3.4 – Hysteretic curves of a) PREG-3 b) APAR-1 and c) COL-1, COL-2 and COL-3

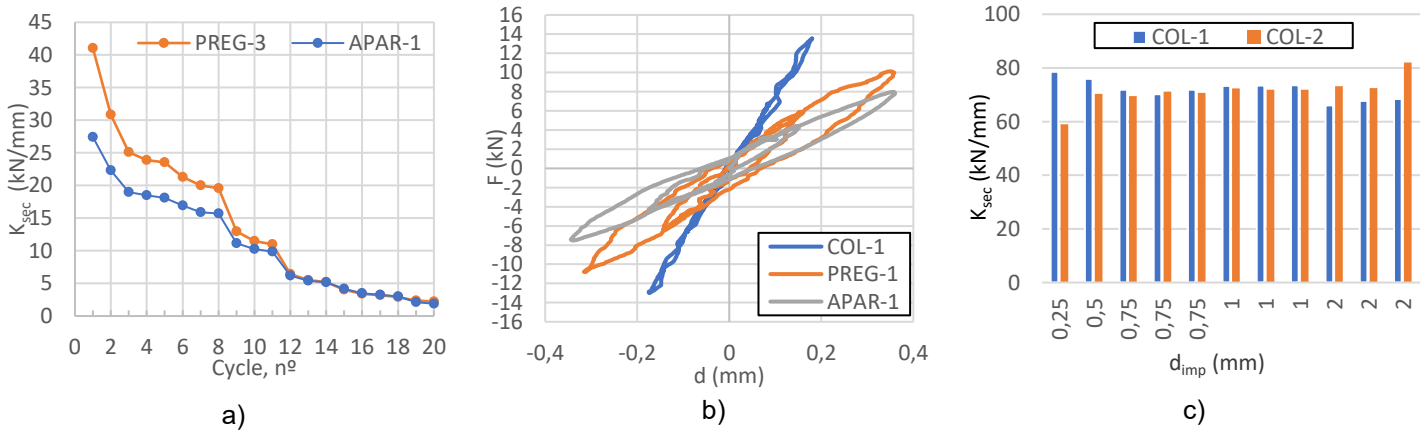

Figure 3.5 – a) Evolution of secant stiffness per cycle b) slipping effect between equipment and testing piece c) Evolution of secant stiffness of glued connections (COL-1 and COL-2)

3.3. Characterization of connections

The envelope behavior of each type of connection was based on the hysteretic curves. For each envelope, it was gathered the values of yielding force and displacement and the values of elastic and plastic stiffness (Figure 3.6). These values were then used to model the tested connections on a numerical software, SAP2000® (CSI V20.0.0).

SAP2000® provides different hysteretic curves, but only the pivot type is able to represent the pinching effect on metal fasteners to some extent. The pivot curve is based on two points that are calibrated from two parameters, α_n and β_n. α_n defines the location of the pivot point according to quadrant n relating it to the elastic stiffness of the structure and the respective yield point; while β_n defines the location of the pinching pivot point that corresponds to the intersection of the discharge curve and the line of elastic stiffness according to quadrant n.

The parameters reached that better suit the metal fasteners connections are stated on the Table 3.2 and the hysteretic curves obtained from the numerical model are presented on Figure 3.7.

Regarding the strength, F_{med}, and secant stiffness, K_{sec} , obtained through the numerical model, it appears that similar values are obtained compared to the laboratory tests (Figure 3.8 a) and b)). However, the model presents lower values of maximum resistance in initial cycles. The secant stiffness is also lower in the first cycles, approaching the real values from cycle nº 8 on (3rd cycle of 1 mm).

When comparing the dissipated energy, E_d, (Figure 3.8 c)), the model shows higher values from cycle nº 20 (3rd cycle of 8 mm) compared to the laboratory tests. Hence why the maximum displacement considered for the connections was 8 mm.

Table 3.2 - Parameters that characterize the specimens' connections in the numerical model

Connection	α_1	α_2	β_1	β_2	F_{ced} (kN)	d_{ced} (mm)	K_{el} (kN/mm)	K_{pl} (kN/mm)
APAR	8	8	0,06	0,06	17,95	1,04	17,21	-0,35
PREG	100	100	0,11	0,11	19,52	0,86	22,79	-0,03
COL	-	-	-	-	-	-	71,61	-

F_{ced} – Yielding force
d_{ced} – Yielding displacement
K_{el} – Elastic stiffness
K_{pl} – Plastic stiffness

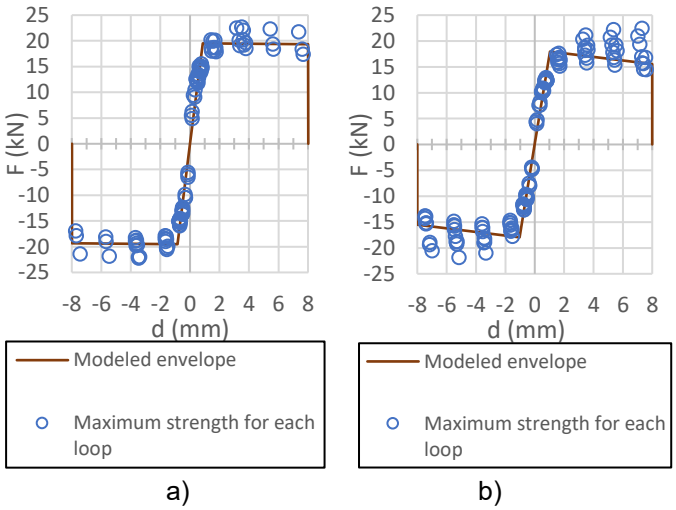

Figure 3.6 – Envelope curve for a) Nailed connections b) Screwed connections

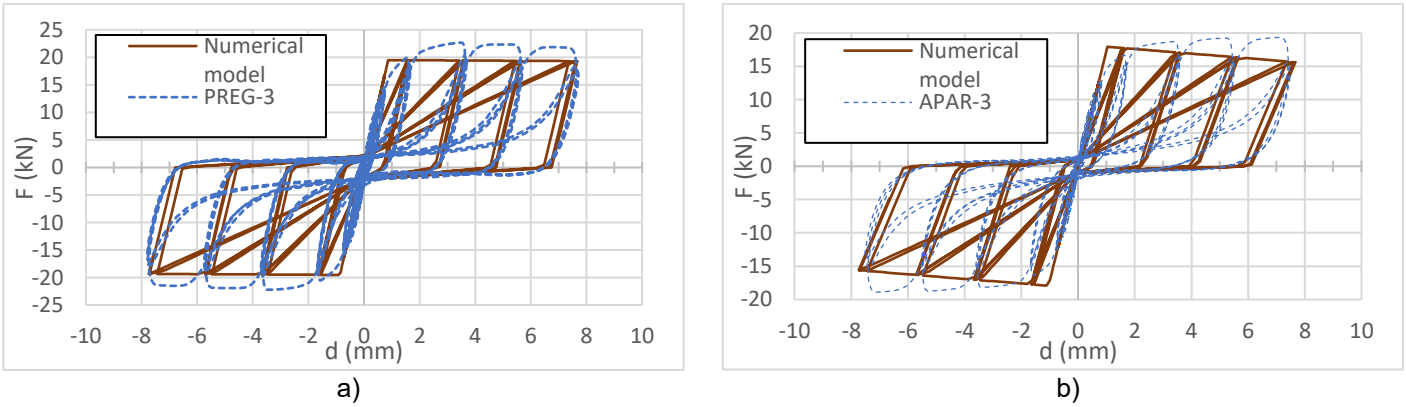

Figure 3.7 – Comparison of hysteretic curves for a) Nailed connections b) Screwed connections

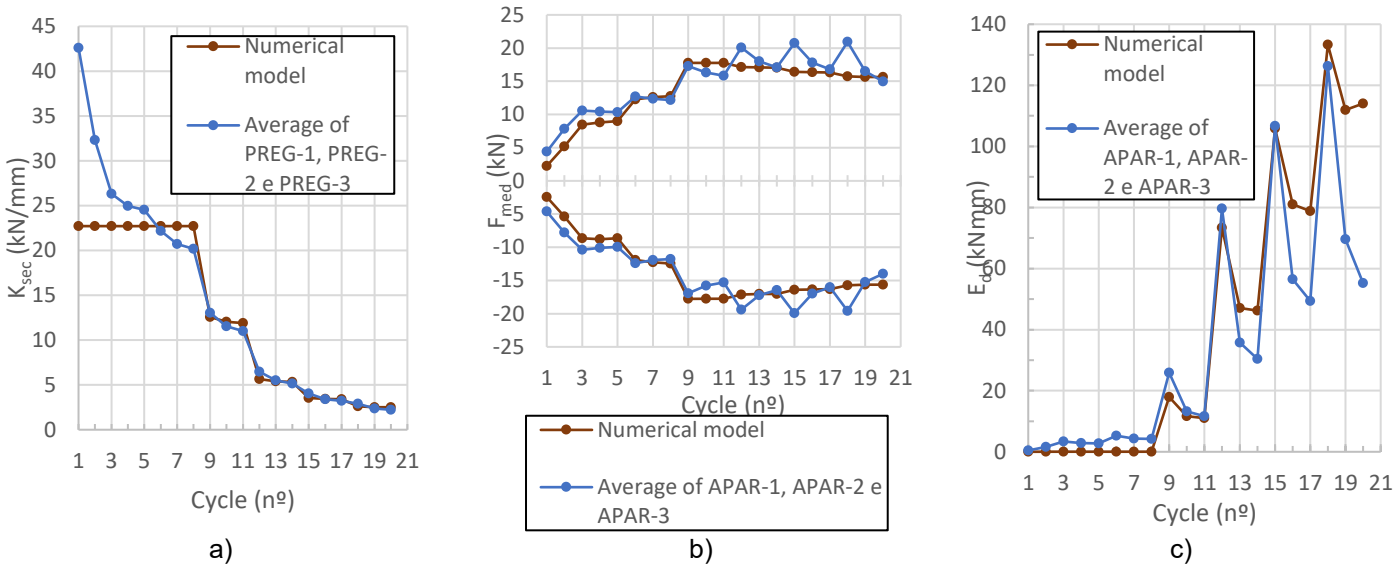

Figure 3.8 – Evolution and comparison between laboratory results (APAR) and numerical model of a) secant stiffness b) Average maximum force c) Dissipated energy

As the test pieces consist of two connections in parallel, the stiffness, K_T, must be changed according to Equation (3.1) in order to represent a single connection, K_{lig}^{ens}. The results are shown on Table 3.3. The same parameters, α_n and β_n, were considered.

$$\frac{1}{K_T} = \frac{1}{K_{lig}^{ens}} + \frac{1}{K_{lig}^{ens}} \Leftrightarrow K_{lig}^{ens} = 2 \times K_T \quad \textbf{(3.1)}$$

Table 3.3 — Parameters that characterize a single tested connection in the numerical model

Connection	α_1	α_2	β_1	β_2	$F_{ced}^{ens.}$ (kN)	$K_{lig,el}^{ens}$ (kN/mm)	$K_{lig,pl}^{ens}$ (kN/mm)
APAR	8	8	0,06	0,06	17,95	34,42	-0,70
PREG	100	100	0,11	0,11	19,52	45,58	-0,06
COL	-	-	-	-	35,81*	143,22	-

(*) Value considering a maximum shear displacement of the testing pieces (2 connections) of 0,5 mm

4. Numerical model of the original floor

The reinforcement proposed on this paper is based on a timber floor executed by Fragomeli (2015) (Figure 4.1). To study the improvement of in-plane stiffness and strength, a model of the original structure was created based on the envelope curve obtained by Fragomeli (2015). Each element was modelled as a finite element of type frame.

Each connection between elements was modelled with non-linear links based on the results of nailed connections and characterized based on the testing results of nailed connections in order to approximate the model envelope curve to the original one (Figure 4.2). Due to the differences (timber density, number and diameter of connectors, number of shear planes) between the connections executed by Fragomeli (2015) and the tested nailed connections, it was necessary to extrapolate the results. EC5-1-1 (2004) recommends the following relation between joints stiffness per connector per shear plane, K_{ser}, and timber mean density, ρ_m, and the diameter of the connector, Φ (Equation (4.1)).

$$K_{ser} = \frac{{\rho_m}^{1,5} \times \Phi}{23} \quad \textbf{(4.1)}$$

The original floor has one connection per intersection between planks and beams and each connection consists of two circular nails spaced by 130,4 mm. This configuration provides joint with rotational stiffness, $K_{torção,el}^{original}$, which was then calculated based on the shear elastic stiffness of each nail.

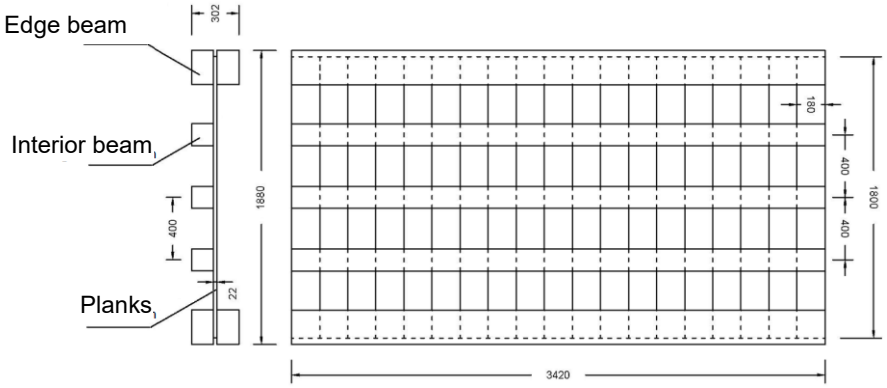

Figure 4.1 – Scheme of the unreinforced floor (Dimensions in mm) (Fragomeli, 2015)

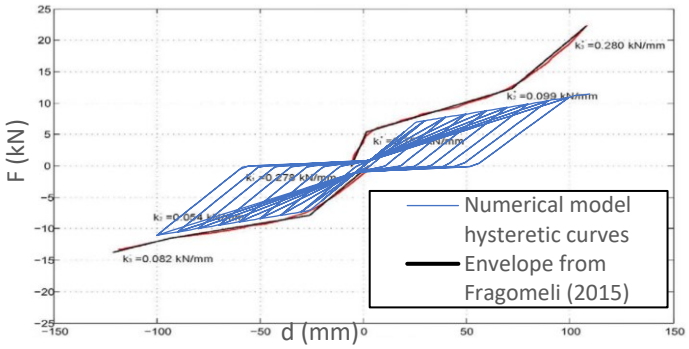

Figure 4.2 – Comparison between the envelope obtain through laboratory testing (Fragomeli, 2015) and the model hysteretic curve

5. Strengthening solution

5.1. Criteria to analyze the solution

Based on experimental results conducted by Vaculik (2012) and Griffith (2006), the maximum admissible in-plane displacement of timber floors, measured in relation to the gable walls, must not exceed 50% of the thickness of the main facade and back walls in order not to promote the overturning of masonry walls.

Nunes (2017) summarized the maximum base shear of three types of old buildings present in the city of Lisbon ("pombalino", "gaioleiro" and "placa" buildings) and the one that shows higher values (32,6 kN/m) is the "gaioleiro" building which was described and characterized by Frazão (2013). The back walls are 400 mm thick on the top floor, the gable walls are spaced by 12,50 m and the floor beams are oriented perpendicularly to the facade (Figure 5.1). These aspects lead to a maximum admissible displacement of 60 mm.

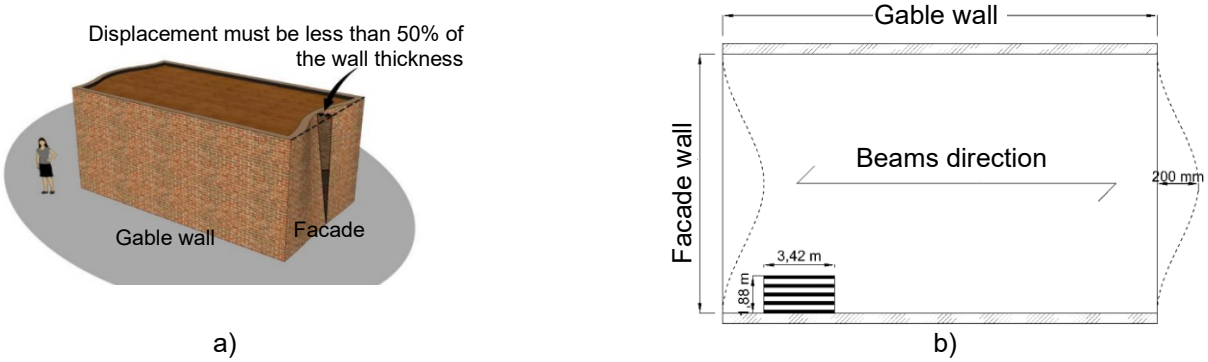

Figure 5.1 – a) Criteria for the maximum displacement in URM buildings (Adaptado de Giongo *et al.* (2014)) b) Schematic geometry of the building and the floor being studied and the respetitive relationship with the maximum allowed displacement.

Thus, it was considered that the reinforced floor must comply with the following criteria:

a) The original elements of the timber floor (planks and beams) must not reach stresses higher than yielding stresses, since timber is a fragile material;

b) The reinforced floor must reach a strength of 111,5 kN (32,6 kN/m x 3,42 m) in an elastic regime without exceeding the maximum limit of 60 mm between edge beams.

5.2. Solution description

The reinforcement is based on oriented strand boards (OSB) of 15 mm thick and a mean density of 550 kg/m^3 which are connected directed to the beams. In order to study the effect of cuts on the panel and the following bridging joints, four different configurations were considered (Figure 5.2). The spacing between connections (50, 75, 100, 150 and 200 mm) and the type of connectors used (nailed or screwed) were also modified between each configuration. Since the glued connections only provided an insight of its elastic stiffness, this type of connection was only used for bridging joints (Figure 5.2 d)). The disposition of connectors followed the scheme shown on Figure 5.2, and the parameters to model each one were based on the tests of timber-to-timber connections. The different configurations are summarized on Table 5.1.

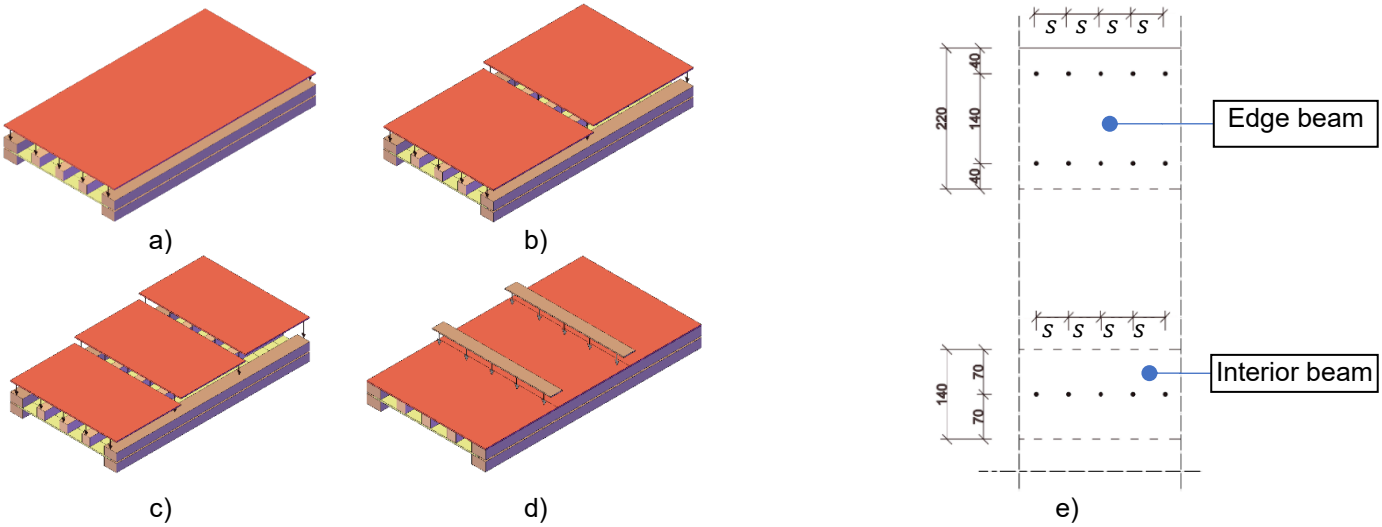

Figure 5.2 – Different confifurations of the same reinforcement: a) One panel (1P) b) Two panels (2P) c) Three panels (3P) d) 3 panels with bridging joints (3P-C) e) Connection scheme between the OSB panel and the beams

Table 5.1 — Name assignment of the different configurations considered as reinforcement

Spacing, s (mm)	Nº of panels	Connector		Bridging joints	
		Screw with an effective diameter of 4 mm	Squared Nail with a side of 4 mm		
50	1	APAR-50-1P	PREG-50-1P	-	-
	2	APAR-50-2P	PREG-50-2P	-	-
	3	APAR-50-3P	PREG-50-3P	APAR-50-3P-C	PREG-50-3P-C
75	1	APAR-75-1P	PREG-75-1P	-	-
	2	APAR-75-2P	PREG-75-2P	-	-
	3	APAR-75-3P	PREG-75-3P	APAR-75-3P-C	PREG -75-3P-C
100	1	APAR-100-1P	PREG-100-1P	-	-
	2	APAR-100-2P	PREG-100-2P	-	-
	3	APAR-100-3P	PREG-100-3P	APAR-100-3P-C	PREG -100-3P-C
150	1	APAR-150-1P	PREG-150-1P	-	-
	2	APAR-150-2P	PREG-150-2P	-	-
	3	APAR-150-3P	PREG-150-3P	APAR-150-3P-C	PREG -150-3P-C
200	1	APAR-200-1P	PREG-200-1P	-	-
	2	APAR-200-2P	PREG-200-2P	-	-
	3	APAR-200-3P	PREG-200-3P	APAR-200-3P-C	APAR-200-3P-C

5.3. Reinforcement results

After the reinforcement system was modeled, a cyclic loading of imposed displacements was applied on the top edge of the floor (Figure 5.3 a)). For each configuration was obtained a hysteric curve which was then used to determine the respective envelope curve (Figure 5.3 b)). From the envelope curve, it was analyzed the elastic stiffness, K_{el}^{Ref}, and the yielding force, F_{ced}^{Ref}.

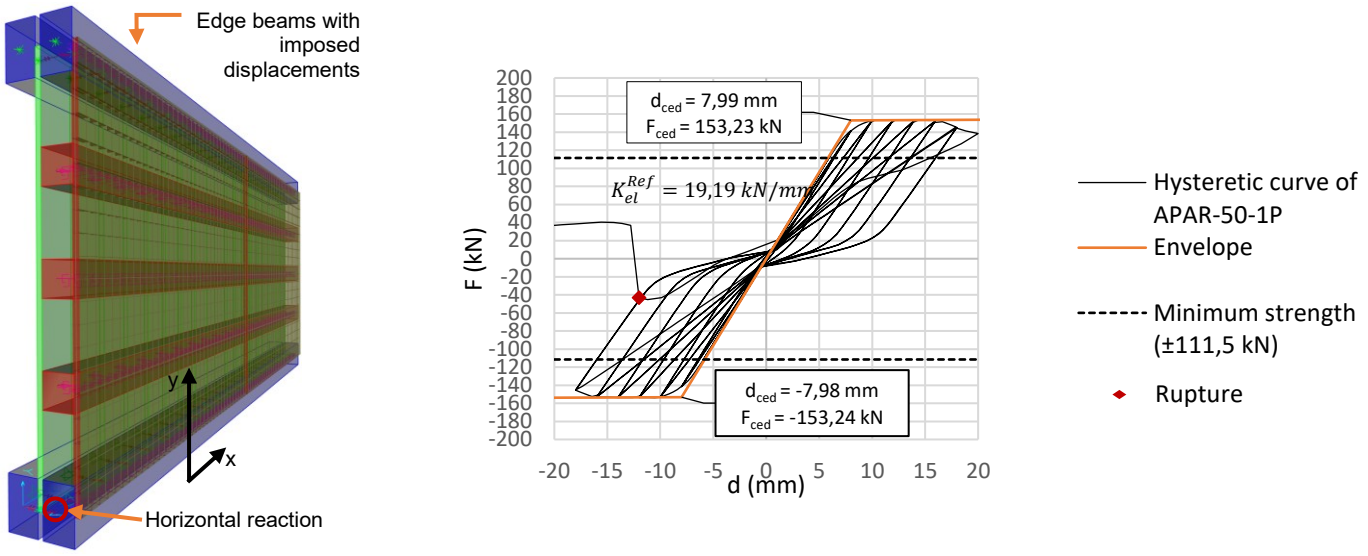

Figure 5.3 – a) Numerical model b) Hysteric curve of APAR-50-1P

To analyze the yield force of each variant, the results of each model were gathered according to the number of connectors used between the upper edge beam and the reinforcement panel (Figure 5.4). These connections are responsible for transmitting the load from the gable walls to the reinforcement system and limiting the resistance of the floor. It was found that for situations where only one OSB panel is used (1P), the yield force is directed related to the connectors yield force as the slope of the linear regression is similar to the these values ($F_{ced}^{1\ screw} = 1{,}12\ kN$ / $F_{ced}^{1\ nail} = 1{,}22\ kN$). However, this relationship is no longer valid as soon as the reinforcement panel is divided. For configurations with 2 panels (2P), the yield force is reduced on average by 25% compared to configurations using a panel and around 50% for configurations with 3 panels (3P). Bridging the joints (3P-C) show similar results to the configurations in which only one panel is used. This could be a solution to avoid discontinuities in the reinforcement and improve its resistance.

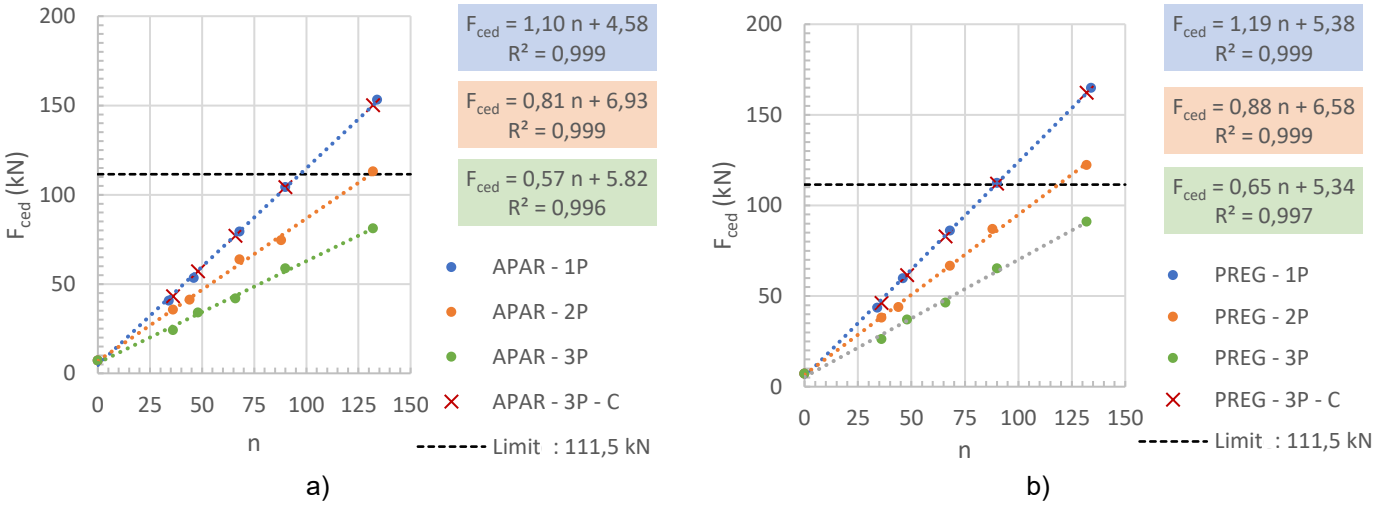

Figure 5.4 –Yielding force as a function of the number of connectors: a) Screwed connections (APAR) b) Nailed connections (PREG)

In terms of elastic stiffness, obtained from the envelope of the hysteretic curves, it appears that the more divisions the reinforcement panel has, the lower the in-plane stiffness of the floor, since the reinforcement system is no longer able to distribute stresses uniformly. However, when bridging the joints, the initial stiffness values remain close to the configurations with one panel. When analyzing the results of all configurations (Figure 5.5), it appears that the panel division has a greater impact on the elastic stiffness than the spacing used in the connections. When checking the loss of in-plane stiffness for APAR-**50**-1P and APAR-**75**-1P variants, this value is around 8%, whereas for APAR-50-**1P** and APAR-50-**2P** it is around 25%. This result is also verified in the configurations in which nailed connections were used. The evolution of elastic stiffness with increasing spacing and increasing the division of the reinforcement panel in relation to configurations with a panel is shown in Figure 5.11. It should also be noted that the nailed connections provide greater rigidity than the screwed connections, agreeing with the results obtained in the laboratory tests described previously.

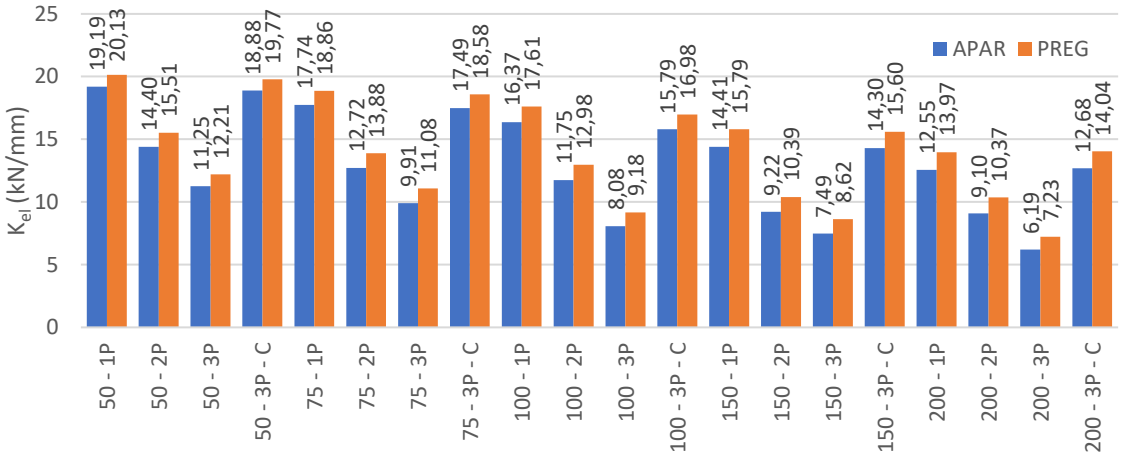

Figure 5.5 – In-plane stiffness of all the reinforcement configurations

6. Conclusions

Eight configurations of the studied solution provide the original floor a substantial improvement of in-plane stiffness, with a minimum increase of 18 times compared to the unreinforced situation. In terms of resistance, there is a minimum increase of 20 times. The results obtained are summarized on Table 6.1, as well as the results presented by Fragomeli (2015). In order to improve the resistance and rigidity of the 2P and 3P configurations without solidifying the joints, the number of connectors should be concentrated close to the panel joints, since these are the areas that condition the resistance and stiffness of the proposed reinforcement. In all the configurations the elements of the floor remain within the elastic regime. Also the yield displacement, when a strength higher than 111,5 kN is reached, guarantees that the maximum floor distortion is low and that will never promote a maximum displacement of the facade of 200 mm out of its plane (Figure 5.1).

Table 6.1 — Results of reinforcements that provide the original floor with adequate in-plane stiffness and strength

Name assignment	Yield force F_{ced}^{Ref} (kN)	Yield displacement d_{ced}^{Ref} (mm)	Elastic stiffness K_{el}^{Ref} (kN/mm)	Plastic stiffness (+) $K_{pl,+}^{Ref}$ (kN/mm)	Plastic stiffness (-) $K_{pl,-}^{Ref}$ (kN/mm)	Equivalent elastic stiffness $(Ge)_{eq}$ (kN/mm)
Pavimento original Fragomeli (2015)	5,38	1,57	0,76	0,099	0,054	0,42
PREG-50-1P	164,86	8,19	20,13	2,18	2,20	11,07
PREG-50-3P-C	162,29	8,21	19,77	2,20	2,23	10,87
PREG-75-1P	112,34	5,96	18,86	2,17	2,16	10,37
PREG-75-3P-C	111,93	6,02	18,58	2,24	2,24	10,21
PREG-50-2P	122,24	7,88	15,51	1,51	1,50	8,53
APAR-50-1P	153,24	7,99	19,19	0,05	0,05	10,55
APAR-50-3P-C	150,13	7,95	18,88	0,28	0,26	10,38
APAR-50-2P	112,96	7,84	14,40	0,52	0,52	7,92

7. References

Brignola, A., Pampanin, S., & Podestà, S. (2012). Evaluation Evoluation of the In-Plane Stiffness of Timber Diaphragms. *Earthquake Spectra, 28*(4), 1687-1709.

Computers and Structures, Inc. (CSI). (2017). *Integrated Solution for Structural Analysis and Design, v20.0.0.* Berkeley, California, USA.

Corradi, M., Speranzini, E., Borri, A., & Vignoli, A. (2006). In-plane shear reinforcement of wood beam floors with FRP. *Composites Part B: Engineering, 37*, 310-319.

EN 12512: Timber Structures - Test Methods - Cyclic Testing of Joints Made with Mechanical Fasteners. (2006). Brussels: European Committee for Standardization (CEN).

Eurocode 5: Design of timber structures - Part 1-1: General - Common rules and rules for buildings. (2004). Brussels: European Committee for Standardization (CEN).

Fragomeli, A. (2015). *Evaluation of an in-plane stiffening technique for ancient timber floors.* Graduation thesis, Universita' Degli Studi Di Pavia, Pavia.

Frazão, M. (2013). *Modelação de um edifício "Gaioleiro" para Avaliação e Reforço Sísmico.* Dissertação de mestrado, Instituto Superior Técnico, Lisboa.

Giongo, I., Wilson, A., Dizhur, D., Derakhshan, H., Tomasi, R., Griffith, M., . . . Ingham, J. (2014). *Bulletin of the New Zealand Society for Earthquake Engineering Vol. 47, No. 2, June 2014*, 97-118.

Griffith, M., Vaculik, J., Lam, N., Wilson, J. L., & Lumantarna, E. (2006). Cyclic testing of unreinforced masonry walls in two-way bending. *Earthquake Engineering and Structural Dynamics*, 801-821.

Instituto Nacional de Estatística. (Julho de 2020). *Censos 2011*. Obtido de Edifícios (N.º) por Localização geográfica (à data dos Censos 2011) e Época de construção; Decenal: https://www.ine.pt/xportal/xmain?xpid=INE&xpgid=ine_indicadores&indOcorrCod=0005967&contexto=bd&selTab=tab2

Nunes, M. B. (2017). *Comportamento de uma solução de reforço metálica para pavimentos de madeira.* Dissertação de mestrado, Instituto Superior Técnico, Lisboa.

Nunes, M., Bento, R., & Lopes, M. (2020). In-plane stiffening and strengthening of timber floors for the improvement of seismic behaviour of URM buildings. *International Journal of Masonry Research and Innovation, 5*(1), 85-120.

Piazza, M., Baldessari, C., & Tomasi, R. (2008). The Role of in-plane floor stiffness in the seismic behaviour of traditional buildings. *The 14th World Conference on Earthquake Engineering.* Beijing, China.

Vaculik, J. (2012). *Unreinforced masonry walls subjected to out-of-plane seismic action.* Tese de douturamento, University of Adelaide, School of Civil, Environmental and Mining Engineering.

Valluzzi, M. R., Modena, C., Benetta, M. D., & Garbin, E. (2010). In-plane strengthening of timber floors for the seismic improvement of masonry buildings. *11th World Conference on Timber Engineering.* Trentino, Italy.